

NEUTRON NOISE SPECTRAL FEATURES OF SIMULATED MECHANICAL AND THERMAL-HYDRAULIC PERTURBATIONS IN A PWR CORE

L.A Torres¹, D. Chionis², C. Montalvo¹, A. Dokhane², A. García-Berrocal¹

¹Energy and Fuels Department, Universidad Politécnica de Madrid (UPM)
Ríos Rosas 21, 28003 Madrid, Spain

²Paul Scherrer Institut, Laboratory for Reactor Physics and Thermal-Hydraulics,
Forschungsstrasse 111, 5232 Villigen-PSI, Switzerland

la.torres@alumnos.upm.es, dionysios.chionis@psi.ch, abdelhamid.dokhane@psi.ch,
cristina.montalvo@upm.es, agustin.garciaberrocal@upm.es

ABSTRACT

KWU-PWR reactors (SIEMENS design) are commonly exhibiting high neutron noise levels that can lead to costly operational issues. Recent analysis seems to indicate that, coolant flow, temperature oscillations, and mechanical vibrations have a key impact on neutron noise phenomena. In order to advance in understanding this phenomenon, the transient nodal code SIMULATE-3K (S3K) has been already utilized to simulate scenarios with individual or combined types of perturbation sources: mechanical vibrations of fuel assemblies and thermal-hydraulic fluctuations at the core inlet. In this work, new simulations are performed with all the perturbations applied simultaneously. The simulated neutron detectors responses are then analyzed with noise analysis techniques. All the simulated spectral features of neutron noise are compared to those obtained from real plant data. Results show that the simulated neutron noise phenomenology behaves similarly to that obtained from real plant data by increasing the fluctuation amplitude in the inlet coolant flow in the S3K calculations.

KEYWORDS: SIMULATE-3K, noise analysis, mechanical vibrations, thermal-hydraulic fluctuations

1. INTRODUCTION

Recently the normalized root mean square (NRMS) of neutron detectors signals have experienced an increase in certain German, Spanish and Swiss pre-Konvoi and Konvoi pressurized water reactors (PWRs) [1-4]. The physical causes behind this raise is under research by many institutions and within the framework of the EU project CORTEX (Core Monitoring Techniques Experimental Validation and Demonstration). Advanced neutron noise modeling using state of the art simulation tools are compared against real plant data within the CORTEX project in order to extract useful spectral features of the underlying phenomena.

In a previous publication [5], used as a basis for the current paper, a series of simulations were performed with the transient 3D nodal code SIMULATE-3K (S3K). All simulations assumed only one type of the following perturbations: fuel bundle vibrations (synchronized vibration of a central cluster of 5x5 assemblies following either a white noise signal or a 1.5 Hz sine wave signal), and coolant flow fluctuations or coolant temperature fluctuations at the core inlet. The simulated data were analyzed by means of noise analysis techniques and several spectral features were found similar to those of the real plant data. The main conclusions from this approach are the following:

- In the scenarios with mechanical vibrations, detectors, located at opposite sides of the direction of the vibration, showed an out-of-phase relationship in the entire frequency range; i.e. a phase distribution dividing the reactor into two halves clearly differentiated by $\pm 180^\circ$. In addition, the phase relationship is zero between detectors located at the different axial levels of the same instrumentation string.
- In the thermal-hydraulic scenarios, two main characteristics were observed. On the one hand, a linear phase difference between neutron detectors located at different axial levels and at the same azimuthal location (due to the transport phenomenon). On the other hand, a high amplitude of the neutron noise spectra below 1 Hz. It has been found also that, the temperature fluctuations are the main cause of the high amplitude of the spectra at low frequency.
- The spectral characteristics of the neutron noise cannot be explained by one single noise source but by a combination of all types of perturbations.

In line with [5-7], the current paper discusses the results obtained from the analysis of several new simulations. The simulated scenarios are based on the combination of two and three types of perturbations, i.e. fuel bundle lateral vibrations, and inlet coolant flow and temperature fluctuations. The amplitude of these perturbations have been modified in every simulation to observe the differences in the spectral characteristics of neutron noise. The final goal is to resemble as much as possible the real plant noise phenomenology and link the spectral characteristics of neutron noise with the physical causes behind it. The current paper presents the most important characteristics obtained from each set of simulations. Due to the high number of simulated scenarios, the observed neutron noise spectral features have been organized properly in order to perform a meaningful assessment.

2. NEUTRON NOISE MODELLING IN SIMULATE-3K

The transient nodal code S3K is used in this work for modelling various types of noise sources and assessing their impact on the neutron noise behavior. To this aim, the PWR core, developed in the framework of the OECD/NEA transient benchmark [8], is modelled using the CASMO5/SIMULATE3/S3K codes sequence. Three types of noise sources are studied in this work by performing transient calculations in S3K. First, fuel assemblies can laterally vibrate, by modifying the water gap widths between the oscillating bundles and their adjacent ones, as described in [9]. In addition to that, the inlet coolant temperature and flow can be imposed to fluctuate in each of the four coolant loops of the core. The transient evolution of the neutron flux is monitored using eight in-core neutron detector instrumentation tubes, which are distributed radially in the core, as presented in Figure 1. Each instrumentation tube contains six in-core neutron detectors, equally distributed in the axial direction. Consequently, the neutron noise spatial distribution, as results from the imposed perturbations, can be estimated and then analyzed using signal and noise analysis techniques, as it is discussed in the next section.

3. SIGNALS AND NOISE ANALYSIS TECHNIQUES

The main tool of noise analysis techniques is based on observing the response of the neutron detector sensors in the frequency domain through the Fourier transform of the autocorrelation function [10], the so-called auto power spectral density (APSD), defined as:

$$APSD(f) = \int_{-\infty}^{\infty} C_{xx}(\tau) e^{-j2\pi f\tau} d\tau \quad (1)$$

being τ the lag used when estimating the autocorrelation function of the sensor output signal $C_{xx}(\tau)$. Analogously, for two variables, we can calculate the cross power spectrum density (CPSD) through the Fourier transform of the cross correlation between both signals:

$$CPSD(f) = \int_{-\infty}^{\infty} C_{xy}(\tau) e^{-j2\pi f\tau} d\tau \quad (2)$$

being C_{xy} the cross correlation between signals x and y . These functions can be used to calculate the signals' pairwise coherence (COH^2) and their phase difference (PHASE), defined as:

$$COH^2(f) = \frac{|CPSD(f)|^2}{APSD_1(f)APSD_2(f)} \quad (3)$$

$$PHASE(f) = \arctg \frac{\text{Im}|CPSD(f)|}{\text{Re}|CPSD(f)|} \quad (3)$$

The coherence function takes values between 0 and 1. A zero coherence means no correlation, whereas, coherence equals one means total correlation. The PHASE is defined as the phase angle difference between the analyzed pair of signals. An in-phase or out-of-phase relationship between the analyzed signals is given by a 0° or 180° phase, respectively.

4. COMBINED PERTURBATIONS SCENARIOS

The simulated scenarios analyzed in the current paper are the following:

- **Scenario A:** This case assumes the combined effect of the fluctuation of the inlet coolant flow and the inlet coolant temperature in all four coolant loops. The inlet coolant flow and inlet coolant temperature are randomly fluctuating with amplitude of $\pm 1\%$ and $\pm 1^\circ\text{C}$, respectively.
- **Scenarios B.1 and B.2:** These two scenarios study the combined effect of the fuel assemblies vibration with Scenario A, i.e. the fluctuation of the inlet coolant flow and the inlet coolant temperature in all the coolant loops. The inlet coolant flow and inlet coolant temperature are randomly fluctuating with amplitude of $\pm 1\%$ and $\pm 1^\circ\text{C}$, respectively. The vibration of the central cluster of 5×5 fuel assemblies, shown in Figure 1, is only in the X-direction and follows a white noise signal (random displacement) with a displacement amplitude of 0.5 mm and 1 mm in Scenarios B.1 and B.2, respectively.
- **Scenarios C.1 and C.2:** These cases are similar to the B scenarios, with the only difference that the vibrating cluster follows a sine wave signal of 1.5 Hz with displacement amplitude of either 0.5 mm (C.1) or 1 mm (C.2).

The last two simulation sets, intent to perform a sensitivity analysis studying the effect of the variation of the amplitudes of the FA vibrations (white noise or sine wave), and the coolant flow and temperature fluctuations on the neutron noise behaviour. To this aim, eight scenarios are considered:

- **Scenario D.1:** $\pm 2\%$, $\pm 1^\circ\text{C}$, white noise signal with a displacement amplitude of 0.5 mm.
- **Scenario D.2:** $\pm 3\%$, $\pm 1^\circ\text{C}$, white noise signal with a displacement amplitude of 1 mm.
- **Scenario D.3:** $\pm 2\%$, $\pm 1^\circ\text{C}$, sine wave signal of 1.5 Hz with a displacement amplitude of 0.5 mm.
- **Scenario D.4:** $\pm 3\%$, $\pm 1^\circ\text{C}$, sine wave signal of 1.5 Hz with a displacement amplitude of 1 mm.
- **Scenario E.1:** $\pm 1\%$, $\pm 2^\circ\text{C}$, white noise signal with a displacement amplitude of 0.5 mm.
- **Scenario E.2:** $\pm 1\%$, $\pm 3^\circ\text{C}$, white noise signal with a displacement amplitude of 1 mm.
- **Scenario E.3:** $\pm 1\%$, $\pm 2^\circ\text{C}$, sine wave signal of 1.5 Hz with a displacement amplitude of 0.5 mm.
- **Scenario E.4:** $\pm 1\%$, $\pm 3^\circ\text{C}$, sine wave signal of 1.5 Hz with a displacement amplitude of 1 mm.

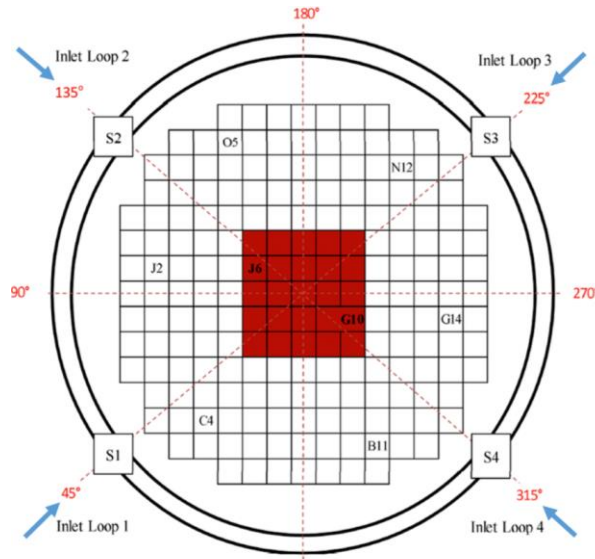


Figure 1: Radial layout of the sensor strings (i.e. O5, N12, J2, J6, G10, G14, C4, and B11), the four inlet coolant loops, and vibrating fuel elements (i.e. red boxes).

5. RESULTS AND DISCUSSION

5.1. Results of Scenario A

The APSD, NRMS distribution, and the coherence and phase functions obtained for Scenario A are very similar to those of the scenario where only temperature fluctuations are assumed [5]. These features are; high values in APSDs for the frequency range below 1 Hz, and high coherence between detectors at the same axial location and linear phase difference with a low slope between detectors at different axial levels at the same instrumentation tube.

5.2. Results of Scenarios B and C

The in-core detectors APSDs at the axial level 5 (level 1 for bottom level; level 6 for top level) for the scenarios B.2 and C.2 are presented in the left and central plots in Figure 2. In addition, the axial detectors NRMS distribution in all radial locations for the scenario B.2 is shown in the right plot in Figure 2. It should be noted that, while only B.2 and C.2 APSDs results are presented here, the results obtained using the scenarios with vibration displacement amplitude of 0.5 mm (B.1 and C.1) have similar trends. The following observations can be made on the APSDs and NRMS:

- The thermal-hydraulic perturbations cause a strong low-frequency spectrum below 1 Hz, as observed in B.2 and C.2 scenarios (i.e. with random and sinusoidal vibrations).
- The neutron noise variance (The area of the APSD) has a similar trend in all the scenarios B and C, and it is directly related to the distance of the in-core detectors from the sources of perturbations (vibrating cluster and the inlet coolant loops).
- In scenarios C (with sinusoidal vibrations), we can see a faster decrease of the APSD as the frequency increases. The random vibrations have a higher response amplitude at high frequencies.
- There is a resonance peak at 1.5 Hz in scenarios C. The largest peak is obtained inside the vibrating cluster (see Figure 2, middle plot).
- The NRMS distribution is very similar in both scenarios B and C, but in real plant data, the axial profile of NRMS is concave with a maximum in the bottom half of the core. [5].
- The NRMS is slightly higher (i.e. 0.1-0.15 % absolute change) in case of 1 mm compared to 0.5 mm displacement of fuel assemblies vibration.

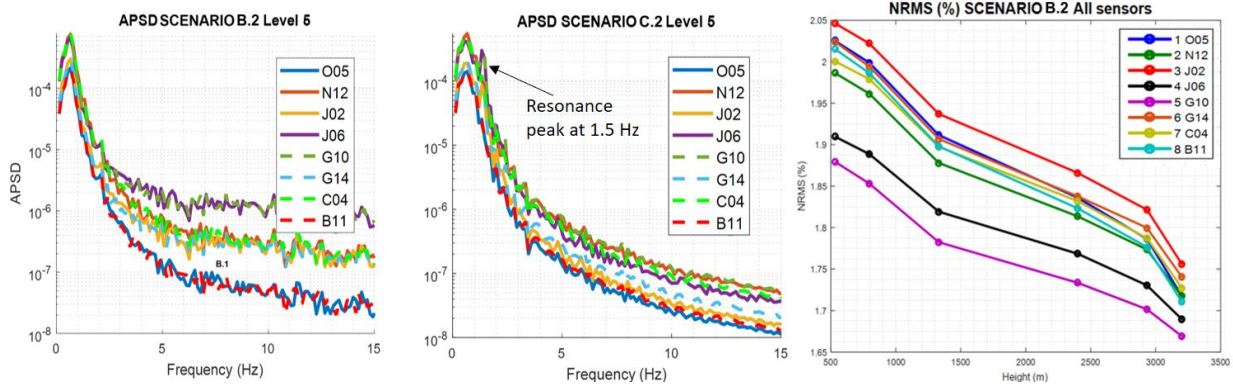


Figure 2: Scenario B.2 (left) and Scenario C.2 (center) APSDs of the radial positions at axial level 5. NRMS of the Scenario B.2 at all radial locations (right).

Regarding the coherence and phase functions in Scenarios C (sinusoidal vibrations), the out-of-phase relationship is only observed at 1.5 Hz, see Figure 3. The rest of the frequency range shows an in phase behavior. Note that, for individual sinusoidal vibrations, the reactor is divided into two zones, but when the thermal-hydraulic oscillations are added, this effect is cancelled out. Also, note that there is only an out-of-phase relationship in Scenarios B above 5 Hz, but with a very low coherence. In addition to that, the larger the amplitude of the vibration is, the lower the frequency at which the out-of-phase relationship starts.

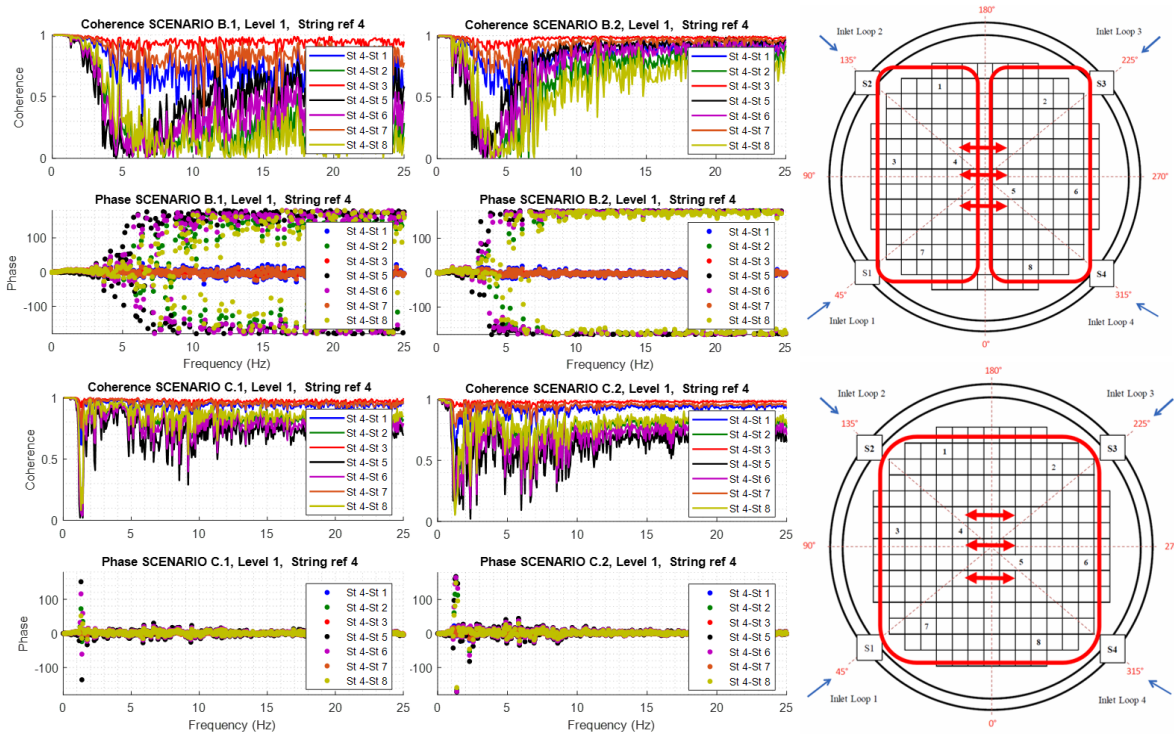


Figure 3: From left to right; Coherence and phase radial distribution. The upper figures correspond to Scenarios B (random vibrations) The lower figures correspond to Scenarios C (sinusoidal vibrations).

In order to explain this behavior, Figure 4 shows the APSD of the in-core detectors at level 1 when individual perturbations are assumed. We can see that below 4 Hz the thermal-hydraulic effect is much larger than the FA random vibration effect. Therefore it is dominant and it drives the whole behavior and this is why the combined effects lead to in-phase behavior. However, above 4-5 Hz the effect of temperature

fluctuations is equal or less than the effect of the mechanical vibrations (APSDs), thus we observe that the phase is shifted towards out-of-phase. When we apply a sine wave vibration of 1.5Hz, we observe the out-of-phase phase because the APSD amplitude due to this mechanical vibration is of the same magnitude, or even larger, of the temperature fluctuations.

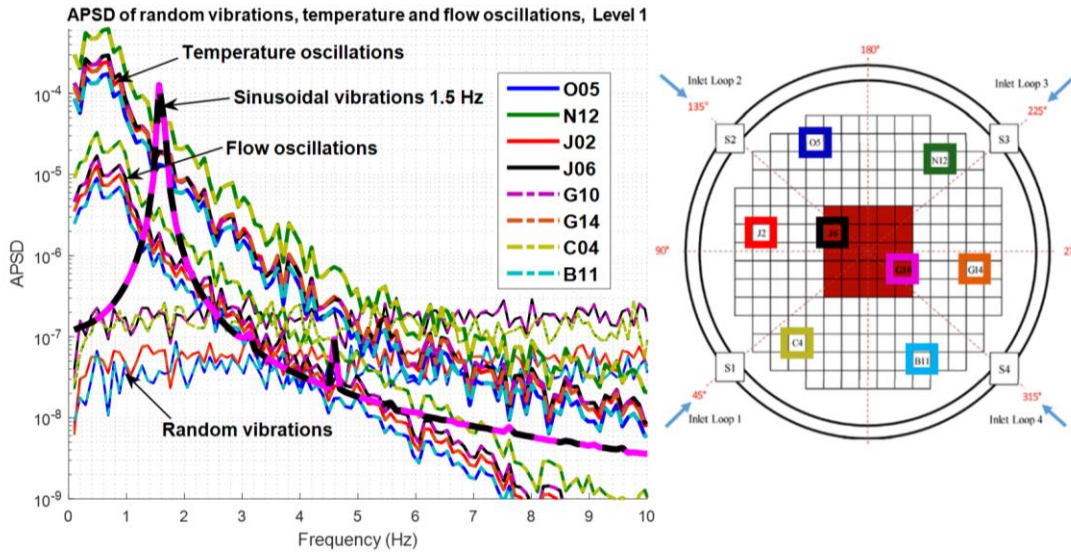


Figure 4: APSD of the simulated response of in-core detectors when individual perturbations are applied.

as a regards to coherence and phase functions between detectors in a same string, Scenarios B and C behave similarly between each other and have similar behavior to that of the scenario with only coolant temperature perturbations. Nevertheless, the slope of the linear phase observed below 1 Hz is higher than that observed in real plant data [5].

5.3. Results of Scenarios D and E

Scenarios D.1 and D.2: The APSDs of Scenarios D.1 and D.2 are very similar to scenarios B.1 and B.2, where most of the energy of the signal is in the low frequency range (i.e. below 1 Hz).

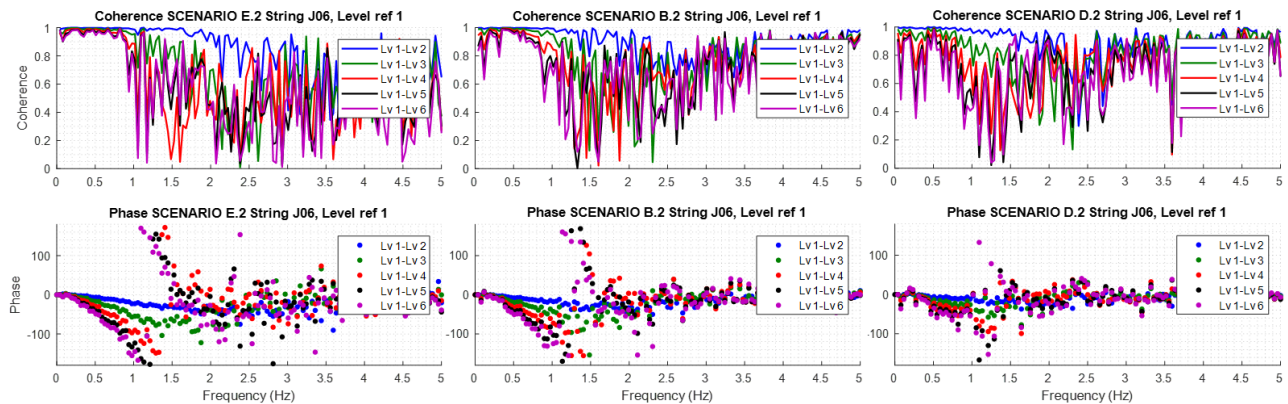


Figure 5: From left to right coherence and phase functions of Scenarios E.2 ($\Delta F \pm 1\%$, $\Delta T \pm 3\text{ }^\circ\text{C}$), B.2 ($\Delta F \pm 1\%$, $\Delta T \pm 1\text{ }^\circ\text{C}$) and D.2 ($\Delta F \pm 3\%$, $\Delta T \pm 1\text{ }^\circ\text{C}$). in all cases random vibrations with amplitude of 1 mm.

Figure 5 from left to right shows how the slope of the linear phase decreases as the relative amplitude of the flow fluctuation increases between detectors in the same string.

Scenarios E.2 ($\Delta F = \pm 1 \%$, $\Delta T = \pm 3 \text{ }^\circ\text{C}$) and B.2 ($\Delta F = \pm 1 \%$, $\Delta T = \pm 1 \text{ }^\circ\text{C}$) present a similar slope, but in D.2 ($\Delta F = \pm 3 \%$, $\Delta T = \pm 1 \text{ }^\circ\text{C}$) the slope decreases. This illustrates the higher sensitivity of the phase slope to the coolant flow fluctuation amplitude compared to that of the coolant temperature fluctuations. By increasing the flow fluctuation amplitude, the neutron noise axial phase relationship becomes more similar to the one observed in real data [5]. Note that, the impact of temperature fluctuations results in a high slope, whereas the effect of flow perturbations results in a low slope on the phase function. Therefore, the combined effect (temperature and flow fluctuations) results in a situation where the value of the slope of the phase function is between the two slopes obtained from the two separate cases. In D.1, the flow fluctuation is lower than in D.2, the effect of the lower slope in the linear phase is not so evident. The radial distribution of the coherences and phases are very similar to scenarios B.1 and B.2. See Figure 2.

Scenarios D.3 and D.4: Regarding the radial distribution of coherences and phase relationships, these scenarios present very similar characteristics as C.1 and C.2, see Figure 3. Nevertheless, for the coherence and phase in the same axial position, we can observe the same behavior presented in Figure 5. The slope of the linear phase decreases as the amplitude of the flow fluctuations increases.

Scenarios E.1 and E.2: The coherence and phase functions in the same axial position show a similar behavior as seen in B.1, with a clear linear phase slope as in the cases with only temperature fluctuations. The radial distribution of coherence and phase functions are very similar to scenario B.1.

Scenarios E.3 and E.4: The coherence and phase functions in the same axial position show a similar behavior as seen in C.1, with a clear linear phase slope as in the cases with only temperature fluctuations. The radial distribution of coherence and phase functions are very similar to scenario C.1.

In general, it is observed that all the APSDs of the Scenarios D.1, D.2, E.1, and E.2 are very similar to scenarios B.1 and B.2, and all the APSDs of the Scenarios D.3, D.4, E.3, and E.4 are very similar to scenarios C.1 and C.2, in which the corresponding spectral peak at 1.5 Hz is evident.

5.4. NRMS Distribution

Figure 6 shows three different NRMS axial profiles. In the left and middle subfigures, we can observe that, when the flow fluctuations are increased up to $\pm 2 \%$ or $\pm 3 \%$ (scenarios D), the profile is almost linear and ascendant. In scenarios B, C and E the NRMS profile are similar to E.2, right subfigure, i.e. almost linear and descendant. In the real case of the reference [5], the neutron noise distribution is concave and with a maximum in the bottom half of the core.

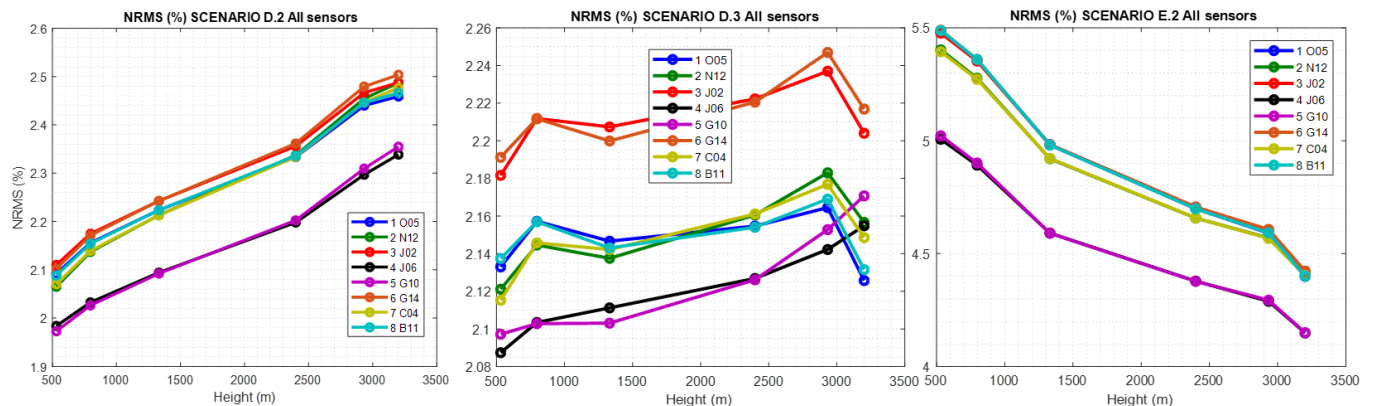


Figure 6: From left to right; Axial NRMS distribution of all sensors for the scenarios D.2 ($\pm 3 \%$, $\pm 1 \text{ }^\circ\text{C}$, random vib. 1mm), D.3 ($\pm 2 \%$, $\pm 1 \text{ }^\circ\text{C}$, 1.5 Hz 1mm) and E.2 ($\pm 1 \%$, $\pm 3 \text{ }^\circ\text{C}$, random vib. 1mm).

6. CONCLUSIONS

The transient nodal code S3K has been used in this paper for the modelling of various noise sources applied simultaneously in the core (i.e. fuel assemblies vibration, inlet coolant flow, and temperature fluctuations). A total number of eleven scenarios are presented in this work. The scenarios differ in the amplitude of the mechanical vibrations and the relative importance of flow and temperature fluctuations. The simulation results are the neutron detectors signals which are analyzed in the frequency domain. The spectral characteristics observed led to the following conclusions:

Mechanical vibrations cause an out-of-phase relationship between opposite detectors in both combined and individual scenarios. This feature has been observed also in real plant data.

In the combined scenarios with both temperature and flow fluctuations, the spectral features of the temperature scenarios are dominant, i.e. high NRMS and high slope in the linear phase between in-core detectors at different axial levels. Nevertheless, there is one type of scenario (3 % flow perturbation, ± 1 °C, and random mechanical vibrations) in which the linear phase slope observed is no longer as the one found in the other scenarios. We cannot firmly state that the slope is lower than in other cases because the linear phase is not well defined, but this case shows that the temperature phenomenon is not so predominant. The NRMS axial profile of the scenario D3 (± 2 %, ± 1 °C, 1.5 Hz 1mm) approaches a convex axial profile that has a similar shape of the one observed when dealing with real plant data.

7. ACKNOWLEDGMENTS

The research leading to these results has received funding from the Euratom research and training program 2014-2018 under grant agreement No 754316 (Project CORTEX Core Monitoring Techniques Experimental Validation and Demonstration).

8. REFERENCES

1. Czibók T, Kiss G, Kiss S, Krinizs K, Végh J. “Regular neutron noise diagnostics measurements at the Hungarian Paks NPP”. *Progress in Nuclear Energy*, vol **43**, pp. 67-74 (2003).
2. Runkel J. *Noise Analysis in Pressurized Water Reactor*. Ph.D. Thesis (1987).
3. Bermejo J, Montalvo C, Ortego A. “On the possible effects contributing to neutron noise variations in KWU-PWR reactor: Modelling with S3K”. *Progress in Nuclear Energy*, vol **95**, pp. 1-7 (2017).
4. Viebach M, Bernt N, Lange C, Hennig D, Hurtado A. “On the influence of dynamical fuel assembly deflections on the neutron noise level”. *Progress in Nuclear Energy*, vol **104**, pp. 32-46, (2018).
5. Torres, L. A., Chionis, D., Montalvo, C., Dokhane, A., & García-Berrocal, A. “Neutron noise analysis of simulated mechanical and thermal-hydraulic perturbations in a PWR core”. *Annals of Nuclear Energy*, vol **126**, pp. 242-252. (2019).
6. D. Chionis, A. Dokhane, H. Ferroukhi, G. Girardin, A. Pautz, “PWR neutron noise phenomenology: Part I – Simulation of stochastic phenomena with SIMULATE-3K”, *Proceedings of the 2018 International Conference on the Reactor Physics (PHYSOR '18)*, Cancun, Mexico (2018).
7. D. Chionis, A. Dokhane, H. Ferroukhi, G. Girardin, A. Pautz, “PWR neutron noise phenomenology: Part II – Qualitative comparison against plant data” *Proceedings of the 2018 International Conference on the Reactor Physics (PHYSOR '18)*, Cancun, Mexico (2018).
8. T. Kozłowski, T. Downar, “*PWR MOX/UO₂ Core Transient Benchmark*”, NEA/OECD (2007).
9. D. Chionis, A. Dokhane, L. Belblidia, M. Pecchia, G. Girardin, H. Ferroukhi, A. Pautz, “SIMULATE-3K analyses of neutron noise response to fuel assembly vibrations and thermal-hydraulics parameters fluctuations”, *Proceedings of the 2017 International Conference on Mathematics & Computational Methods Applied to Nuclear Science & Engineering (M&C '17)*, Jeju Korea, April 16th-20th (2017).
10. Newland, D.E., *An Introduction to Random Vibrations, Spectral and Wavelet Analysis*. Dover Publications, Incorporated (2012).